https://doi.org/10.5194/egusphere-2024-3161
Preprint. Discussion started: 13 November 2024
© Author(s) 2024. CC BY 4.0 License.

Evaluating the accuracy of downwind methods for quantifying point source emissions

Mercy Mbua*[,1], Stuart N. Riddick[1], Elijah Kiplimo[1] and Daniel Zimmerle[1]

[1]*The Energy Institute, Colorado State University, CO, 80524, Fort Collins, USA*

**Correspondence to*: Mercy Mbua (Mercy.Mbua@colostate.edu)

Abstract. The accurate reporting of methane (CH_4) emissions from point sources, such as fugitive leaks from oil and gas infrastructure, is important for evaluating climate change impacts, assessing CH_4 fees for regulatory programs, and validating methane intensity in differentiated gas programs. Currently, there are disagreements between emissions reported by different quantification techniques for the same sources. It has been suggested that downwind CH_4 quantification methods using CH_4 measurements on the fence-line of production facilities could be used to generate emission estimates from oil and gas operations at the site level, but it is currently unclear how accurate the quantified emissions are. To investigate model accuracy, this study uses fence-line simulated data collected during controlled release experiments as input for eddy covariance, aerodynamic flux gradient and the Gaussian plume inverse methods in a range of atmospheric conditions. The results show that both the eddy covariance and aerodynamic flux gradient methods underestimated emissions in all experiments. Although calculated emissions had significant uncertainty, the Gaussian plume inversion method performed better. The uncertainty was found to have no significant correlation with most measurement variables (i.e. downwind measurement distance, wind speed, atmospheric stability, or emission height), which indicates that the Gaussian method can randomly either underestimate or overestimate emissions. For eddy covariance, downwind measurement distance and percent error had negative correlation indicating that far away emissions sources were likely underestimated or be undetected. The study concludes that using fence-line measurement data as input to eddy covariance, aerodynamic flux gradient or Gaussian plume inverse method to quantify CH_4 emissions from an oil and gas production site is unlikely to generate representative emission estimates.

1 Introduction

Methane (CH_4), the primary component of natural gas (NG), is a potent greenhouse gas with a global warming potential of 27 carbon dioxide (CO_2) equivalent over 100 years (US EPA, 2016). Methane emissions reduction is a key part of global initiatives to reduce climate change (Chung, 2021). The 2021 Global Methane Assessment by the Climate and Clean Air Coalitions (CCAC, 2024) and the United Nations Environment Programme (UN Environment Programme, 2024) state that reducing CH_4 emissions from anthropogenic sources by 45% in 2030 would result in avoiding a global atmospheric temperature increase of 0.3°C in 2045 (Chung, 2021). Such measures would align with the Paris Agreement goal of limiting global temperature rise to 1.5˚C by 2030 (United Nations Climate Change, 2015). The US is one of the countries that reports its total greenhouse gas emissions to the Intergovernmental Panel on Climate Change as part of the Paris Agreement (United Nations Climate Change, 2015).

Currently, the amount of CH_4 emitted from US oil and gas production is calculated by the US Environmental Protection Agency (EPA) using a bottom-up inventory approach. The inventory approach multiplies emission factors

© Author(s) 2024. CC BY 4.0 License.

(CH_4 emissions per equipment e.g., separator or emissions per event e.g., liquid unloading) by activity factors (total number of pieces of equipment or events (OAR US EPA, 2023)). This quantification approach has several shortcomings, including: 1. It separately calculates CH_4 emissions from natural gas and petroleum systems, which practically are not independent systems, and can result in bias based on changes in gas to oil ratios throughout a basin (Riddick et al., 2024a); 2. Some emission factors used are outdated (Riddick et al., 2024b) and others do not account for the temporal and spatial variation in emissions (Riddick and Mauzerall, 2023); and 3. Emission factors do not account for the long-tail distributions in emissions distributions (Riddick et al., 2024b). Recently, mechanistic models, such as the Colorado State University's Mechanistic Air Emissions Simulator (MAES), have been developed to address shortcomings in bottom-up CH_4 reporting (Colorado State University, 2021) but these still depend on direct measurements to inform emission factors.

Top-down methods, including using aircraft and satellites, can also be used to infer emissions. For example, Carbon Mapper satellites can locate and quantify CH_4 emissions using absorption spectra taken from space (Carbon Mapper, 2024). However, these survey methods only quantify emissions over a very short period of time (< 10 s) and observations are typically made during the day which can often coincide with maintenance activities that can bias emissions and result in overestimation (Riddick et al., 2024a; Zimmerle et al., 2024). Additionally, different top-down technologies measuring the same source have disagreed in their reported emissions which has called into question the credibility of these methods (Brown et al., 2023; Conrad et al., 2023). As a result, ensuring accuracy in models and technologies used in CH_4 emissions quantification has been a complex issue.

The accurate reporting of CH_4 from fugitive emissions at oil and gas production sites is important for evaluating potential effects on climate change, correctly assessing CH_4 fees on companies as part of the Methane Emissions Reduction Program created under the 2022 Inflation Reduction Act (OA US EPA, 2023), and validating CH_4 content of reported differentiated gas composition where NG companies differentiate their market products based on the environmental impact (CO2EFFICIENT, 2022). Direct measurements have been recommended to augment/update emissions factors used in bottom-up inventories and for better understanding temporal/spatial variability of emissions (Riddick et al., 2024). Downwind methods are widely used to directly measure CH_4 emissions from area and point sources at site/basin levels due to their low cost and wide coverage within a short time (Caulton et al., 2018; Heimburger et al., 2017; Riddick et al., 2020, 2022a; Sonderfeld et al., 2017). Commonly used downwind quantification methods include the Gaussian plume inversion method, eddy covariance, backward Lagrangian stochastic models, aerodynamic flux gradient, mass balance method, the EPA Other Test Method (OTM 33) and the Gaussian puff modelling approach (Denmead, 2008; Edie et al., 2020; Foster-Wittig et al., 2015; Jia et al., 2023; Kamp et al., 2020; Nemitz et al., 2018; Shaw et al., 2021).

Currently, fence-line methods are used to detect, localize and quantify emissions. This approach uses point sensors fixed to the fence-line of the production site and emissions detected when the measured concentration exceeds a threshold, localized by triangulating multiple detections and quantified using a simple dispersion modelling framework, usually based on a Gaussian plume approach (Bell et al., 2023; Day et al., 2024; Jia et al., 2023; Riddick et al., 2022a). The detection and localization of simulated fugitive emission have been successful, with controlled release testing against point sensors and scanning/imaging solutions reporting a 90% probability of detection for

https://doi.org/10.5194/egusphere-2024-3161
Preprint. Discussion started: 13 November 2024
© Author(s) 2024. CC BY 4.0 License.

emission of between 3.9 and 18.2 kg CH_4 h^{-1} (Ilonze et al., 2024). Major shortcomings have been identified using a fence-line approach with quantified emissions reported at between a factor of 0.2 to 42 times for emissions between 0.1 and 1 kg CH_4 h^{-1}, and between 0.08 and 18 times for emissions greater than 1 kg CH_4 h^{-1} (Ilonze et al., 2024). As a result, questions have arisen if other approaches, such as the eddy covariance or aerodynamic flux gradient would generate more accurate results. These methods have been suggested as they have been used to quantify emissions from other sectors, i.e. agriculture (Denmead, 2008; Morin, 2019) and landfills (Xu et al., 2014), have been used to quantify emissions in large downwind areas (Vogel et al., 2024), and quantification does not require assumptions made on downwind dispersion coefficients or micrometeorology that are often required for dispersion modelling (Denmead, 2008).

Due to interest in using a subset of these methods to quantify emissions from oil and production sites, this study will evaluate the quantification accuracy of the eddy covariance, aerodynamic flux gradient, and Gaussian plume inverse methods. Eddy covariance is a vertical flux gradient measurement that measures CH_4 emissions based on the covariance between CH_4 concentrations measured using a fast-response analyzer (> 10 Hz) and vertical wind vector measured by a fast-response sonic anemometer (>10 Hz) (Figure 1A; Morin, 2019). It is typically implemented over long homogenous fetches where eddy mixing scale is a small fraction of the distance from the site providing more predictable vertical transport. The aerodynamic flux gradient method quantifies CH_4 emissions from a source by comparing CH_4 concentrations at two heights (Figure 1B; Querino et al., 2011). The Gaussian Plume Inverse method calculates CH_4 mole fraction at a point in space (x, y, z) as a function of the downwind distance, perpendicular distance (crosswind), mean wind speed and atmospheric stability (Jia et al., 2023; Riddick et al., 2022b). These approaches were developed to quantify emissions from single-point or area emission sources and have not been tested against a controlled release to evaluate their quantification performance. The aerodynamic flux gradient and eddy covariance, for example, have been used to measure trace gas, e.g., nitrogen oxide and carbon dioxide, fluxes from large croplands (Kamp et al., 2020).

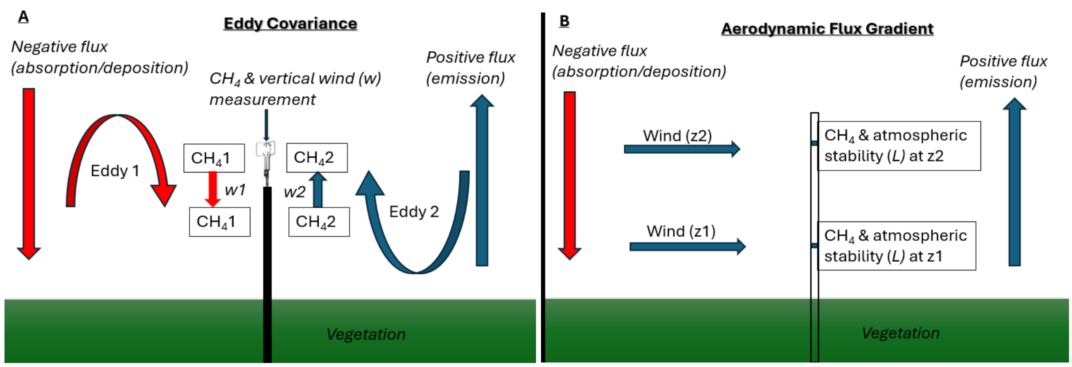

Figure 1: Illustrations of eddy covariance (A) and flux gradient measurements (B) where CH_4 is methane concentrations, *w* is the vertical wind speed, *L* is the Monin-Obukhov length (measure of atmospheric stability), and z is the measurement height.

The Gaussian plume inversion method has been used to quantify emissions from oil and gas production sites (Caulton et al., 2014; Riddick et al., 2022b) but it assumes a homogenous, steady state flow, uniform dispersion of gas in an

https://doi.org/10.5194/egusphere-2024-3161
Preprint. Discussion started: 13 November 2024
© Author(s) 2024. CC BY 4.0 License.

open area free of obstructions (Hutchinson et al., 2017). Oil and gas emissions are characterized by intermittent, non-uniform, single or multiple point source emissions, varying in leak size, location, height and distance between the source and sensor, and are typically in complex aerodynamic environments (i.e. not flat). The need for accurate CH_4 quantification and reporting necessitates evaluating the performance of these downwind quantification approaches in different controlled release and characterized meteorological conditions, to ensure credibility.

This study aims to investigate the performance of these methods in quantifying emissions for known gas release rates and evaluating uncertainties that could result in incorrect CH_4 reporting. Specifically, the study will (1) evaluate the overall quantification accuracy of eddy covariance, aerodynamic flux gradient, and the Gaussian plume inverse method in quantifying single-point and multi-point emissions that simulate oil and gas emissions, (2) evaluate the probability of these models quantifying within a defined range (i.e. ±30%), and (3) investigate which variables have the largest effect on quantification uncertainty.

2 Methods

2.1 Experimental Setup

Controlled release experiments were conducted at the Colorado State University's Methane Emissions Technology Evaluation Center (METEC) in Fort Collins, CO, USA, between February 8, and March 27, 2024. The weather conditions during the test period were mostly sunny but precipitation was also observed (32 sunny, 7 snowy, 12 rainy, 7 cloudy and 1 foggy day; Supplementary Information Section 1). Wind speeds were between 0 and 25 m s^{-1} and temperatures ranged between -15 and +19 °C (Supplementary Information Section 1). Two stationary masts holding the instrumentation were setup on the North-West corner of METEC to take advantage of the predominant wind direction, avoid the largest aerodynamic obstructions and to simulate the likely placement of a fence line instrument (Figure 2; Day et al., 2024; Riddick et al., 2022a). Fenceline sensors are typically placed within the oil and gas perimeter (~30 m) (Riddick et al., 2022a). This study collected data for both close and far away releases, distances between 9 and 94 m.

https://doi.org/10.5194/egusphere-2024-3161
Preprint. Discussion started: 13 November 2024
© Author(s) 2024. CC BY 4.0 License.

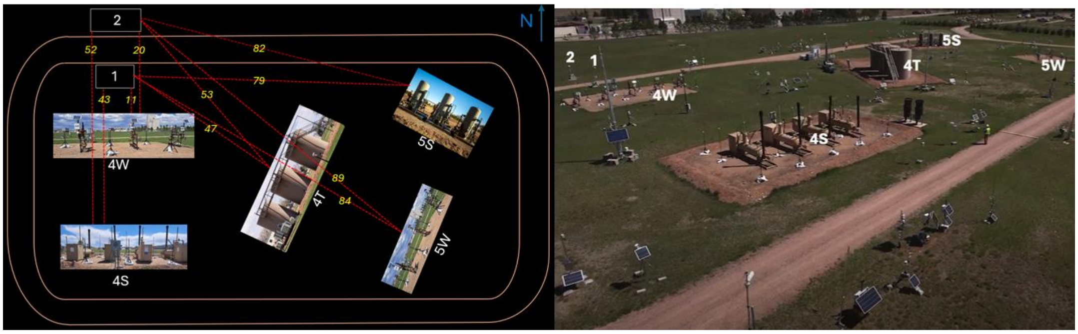

Figure 2: Left pane: Map illustration of major pieces of equipment and the measurements points at Colorado State University's Methane Emissions Technology Evaluation Center (METEC) in Fort Collins, CO, USA. 4S denotes the location of horizontal separators, 4W are well heads, 4T are tanks, 5S are vertical separators and 5W are well heads. 1 is the measurement point for the Microportable Greenhouse Gas Analyzer and 2 is the measurement point for the Aeris analyzers. The red dotted lines with yellow numbers show the average distances (meters) between emission equipment and measurement points. Right pane: Image of METEC showing relative heights of equipment ("METEC | Colorado State University," 2024).

To calculate emissions using the aerodynamic flux gradient approach, two sampling inlets were mounted at 2 and 4 m heights on mast 2 and connected to the inlets of two Aeris (Hayward, CA, USA) MIRA Ultra Series analyzers (Figure 3A). The analyzers were housed in a temperature-controlled unit and sampled at 5 Hz. Data from the 2 m analyzer were also used as input for the Gaussian Plume Inverse method analysis. To collect CH_4 concentration data for the eddy covariance method, the inlet tubing of the ABB (Zurich, Switzerland) GLA131 Series Microportable Greenhouse Gas Analyzer (MGGA) sampling at 10 Hz was collocated with an R. M. Young (Traverse City, MI, USA) 81000 sonic anemometer (R.M. Young Company, 2023) which measured micrometeorology at 10 Hz, 3 m height above ground level on mast 1 (Figure 3B).

https://doi.org/10.5194/egusphere-2024-3161
Preprint. Discussion started: 13 November 2024
© Author(s) 2024. CC BY 4.0 License.

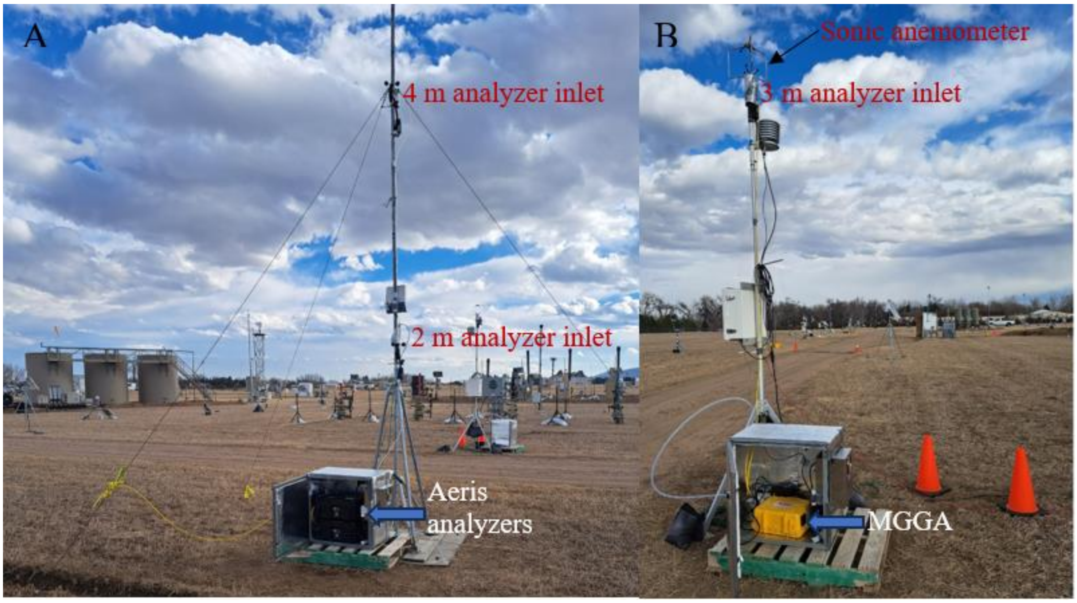

Figure 3: A is the aerodynamic flux gradient and Gaussian plume inverse sampling points and B is the eddy covariance sampling point. The two sampling points are 9.4 m apart.

2.2 Controlled Methane Releases

At METEC, natural gas of known CH_4 content was released from above-ground emission points attached to equipment typically present in an oil and gas facility (tanks, separators and well pads). The gas release rates ranged between 0.005 kg h^{-1} and 8.5 kg h^{-1}, and the release durations ranged from 10 seconds to 8 hours, simulating both fugitive and large emission events. The releases were run both during the day and night. The distance from the release points to the measurement points ranged between 9 and 94 m, and emission heights were between 0.4 and 6.9 m (Figure 2). Emission points simulate the realistic size and locations of typical emission from components such as the thief hatches, pressure relief valves, flanges, bradenheads, pressure transducers, Kimray valves and vents. The releases included both single point emissions (single releases) and multi-point emission events (multiple simultaneous releases).

2.3 Data Processing

Methane concentrations data from the analyzers were aggregated with the meteorological data from the sonic anemometer. For aerodynamic flux gradient and Gaussian plume inverse method data were averaged to 1 Hz, for the eddy covariance the raw CH_4 10 Hz data was used. The aggregated meteorological-concentration data were then merged with METEC's release data and metadata, and event tables created. The meteorological-concentration-release event data were then separated into single-point and multi-point events. The event tables were split into 20-minute emission events for aerodynamic flux gradient and Gaussian plume inverse method as they are dependent on atmospheric stability that is typically determined in time durations of 15 to 30 minutes. Shorter duration measurements (i.e. <15 minutes) may not represent the mean atmospheric state, while longer periods (> 30 minutes) may cause errors especially during rapid transitions in weather conditions (Crenna, 2006). 30-minute events were used for eddy

© Author(s) 2024. CC BY 4.0 License.

covariance processing following published typical averaging times of eddy covariance measurements (Nemitz et al., 2018), and its quantification is assumed to be independent of atmospheric stability (Denmead, 2008).

For eddy covariance and aerodynamic flux gradient, Monin-Obukhov length (*L*) was calculated as the measure of atmospheric stability for every 20 or 30-minute time period, depending on the method, using output from the sonic anemometer. *L* was calculated from the surface friction velocity (u_*, m s^{-1}), mean potential temperature (Θ, K), von Kármán's constant (*k*, 0.41), gravitational acceleration (*g*, 9.8 m s^{-1}) and the surface (kinematic) turbulent flux of sensible heat w'Θ' (Eq. 1 and 2) (Kljun et al., 2015; Stull, 1988).

$$L = -\frac{u_*^3\Theta}{k_v g \overline{w'\Theta'}} \tag{1}$$

$$u_* = \left[\left(\overline{u'w'}\right)^2 + \left(\overline{v'w'}\right)^2\right]^{1/4} \tag{2}$$

For the Gaussian method, atmospheric stability was calculated based on the EPA standard operating procedure for point source Gaussian method (US EPA, 2013). The average local wind stability class (*pgi*) was calculated as the average of atmospheric stability determined using the standard deviation of the wind direction, and the stability calculated from turbulent intensity (ratio of the standard deviation of the wind speed to the average wind speed). The dispersion coefficients used for Gaussian quantification were extracted from the EPA operating procedure that provided coefficients for distances ranging from 1 to 200 m from source (US EPA, 2013).

The wind direction (*WD*) and speed (*WS*) were calculated from the wind vectors u and v, based on the manufacturer's configuration: +*u* values = wind from the east, +*v* values = wind from the north, and +*w* = updraft (Eq. 3 and 4).

$$WD = \mathrm{mod}(90 - \mathrm{atan2d}(v, u), 360) \tag{3}$$

$$WS = \sqrt{u^2 + v^2} \tag{4}$$

The bearing of each release point to the masts' location was calculated using the latitudes and longitudes of the release points provided in the METEC metadata. This bearing was used to determine when the masts were downwind of the release points during the 20/30-minute period. The models' quantification accuracies were tested in three downwind ranges: ±10°, ±20°, and ±30°. A mast was considered downwind when the wind direction was within the specified range for 30% of the 20/30-minute duration. Results for the 20-degree range are presented in the Results section, while the 10- and 30-degree results are included in the Supplementary Material. The 30% threshold was chosen to ensure sufficient data points for evaluating the models. The data were categorized into single release single emission (single emission at the site and the mast was downwind of the release point), multi release single emission (multiple emissions at the site level, but the mast was downwind of a single release point), and multi release multi emission (multiple emissions at the site level, but the mast was downwind of more than one release point).

https://doi.org/10.5194/egusphere-2024-3161
Preprint. Discussion started: 13 November 2024
© Author(s) 2024. CC BY 4.0 License.

2.4 Methane Emissions Quantification

2.4.1 Background Concentration

Background concentration was determined for each of the sensors to calculate CH_4 enhancement. Due to inherent variation in sensors that were used in this study, CH_4 background was calculated for each sensor separately. CH_4 background was calculated as the average of the lowest 5th percentile of all continuous concentration readings (US EPA, 2013). Methane enhancement was determined as CH_4 concentration measurement minus the background concentration measurement.

2.4.2 Eddy Covariance

Emissions were quantified using the eddy covariance method for all three emissions scenarios (single release single emission, multi release single emission and multi release multi emission). Methane flux (F, kg m^{-2} s^{-1}) was calculated as the covariance between the vertical wind speed (w, m s^{-1}) and CH_4 enhancement (c, g m^{-3}) over 30 minutes (Eq. 5; Denmead, 2008).

$$F = w'c' \tag{5}$$

2.4.3 Aerodynamic Flux Gradient

Aerodynamic flux gradient quantification was also tested in all three cases. Methane flux (F, kg m^{-2} s^{-1}) was calculated based on surface friction velocity (u_*, m s^{-1}), von Kármán's constant (k_v, 0.41), the difference in the average CH_4 enhancement between the higher and lower height (g, m^{-3}), natural log of the higher and lower height, and stability correction factors Ψ (Eq. 6; Denmead, 2008; Kamp et al., 2020).

$$F = \frac{u_* k_v (c_2 - c_1)}{In\left(\frac{z_2}{z_1}\right) - \Psi_{c,2} + \Psi_{c,1}} \tag{6}$$

2.4.4 Determining the Area of Vertical Flux Contribution

Eddy covariance and aerodynamic flux gradient measurements at a point (0, 0, z) generate vertical fluxes in kg m^{-2} s^{-1}. In this study, these fluxes represent emissions from single-point or multi-point sources distributed over an area (m^2). The Kljun et al. (2015) footprint model, was used to calculate footprint, and determine the area that contributed 80% (r = 80, $10 \leq r \leq 90$) of the vertical flux measured by the eddy covariance and aerodynamic flux gradient systems. In previous studies, 80% footprints have been used due to the difficulty of reproducing 90% of the sources under neutral and stable conditions, where footprints tend to be long. The difference between the 80% and 90% contours is typically excessively large, despite minimal flux contributions in that area (Rey-Sanchez et al., 2022). The Kljun et al. (2015) model calculates footprint as a function of effective height (z_m = sensor height (z) – displacement height (m)), roughness length (z_o, m) / mean wind speed (u_{mean}, m s^{-1} - used in this study), height of the boundary layer (h, m), Obukhov length (L, m), standard deviation of the lateral velocity (σ_v, m s^{-1}), and friction velocity ($u*$, m s^{-1}) (Kljun et al., 2015). The roughness sublayer in the model was set to 1 (footprint is calculated even if z_m is within the roughness layer). The area of vertical flux contribution was calculated as the polygon area covered by the contour. Due to the limitations of the flux footprint model for the measurement height and stability (Kljun et al., 2015), 20/30-minute files flagged by the footprint model when $z_m/L < -15.5$, were excluded from further analysis.

https://doi.org/10.5194/egusphere-2024-3161
Preprint. Discussion started: 13 November 2024
© Author(s) 2024. CC BY 4.0 License.

2.4.5 Gaussian Plume Inverse Method

The Gaussian plume inverse method was used to quantify single release single emission and multi release single emission. The quantified emission (Q, kg h^{-1}) was calculated from the CH_4 enhancement (X, g m^{-3}), wind speed (u, m s^{-1}), horizontal dispersion coefficient (σ_y, m), vertical dispersion coefficient (σ_z, m), crosswind distance (y, m), sampling height (z, m), emission height (h_s, m), and the height of the boundary layer (Equation 7; Riddick et al., 2022b).

$$X(x,y,z) = \frac{Q}{2\pi u \sigma_y \sigma_z} e^{-\frac{y^2}{2\sigma_y^2}} \left(e^{\frac{-(z-hs)^2}{2\sigma_z^2}} + e^{\frac{-(z+hs)^2}{2\sigma_z^2}} + e^{\frac{-(z-2h+hs)^2}{2\sigma_z^2}} + e^{\frac{-(z+2h-hs)^2}{2\sigma_z^2}} + e^{\frac{-(z-2h-hs)^2}{2\sigma_z^2}} \right) \tag{7}$$

3 Results

3.1 Methane Emission Quantification

3.1.1 Eddy Covariance

For stable, continuous 30-minute release events, emissions calculated using the eddy covariance method were an underestimate for single release single emission, multi release single emission and multi release multi emission events (Figure 4). All data points were below the 1:1 line. A plot of the quantified emission versus controlled release (kg h^{-1}) did not show a linear correlation (R^2 between 0.03 and 0.36), as all emissions were largely underestimated. The eddy covariance method reported emissions of between 0 and 0.5 kg h^{-1} overall, despite actual emissions being between 0 and about 7 kg h^{-1} (Figure 4). The underestimation was consistent across all downwind ranges, 10, 20 and 30 degrees (Supplementary Material Section 2.1).

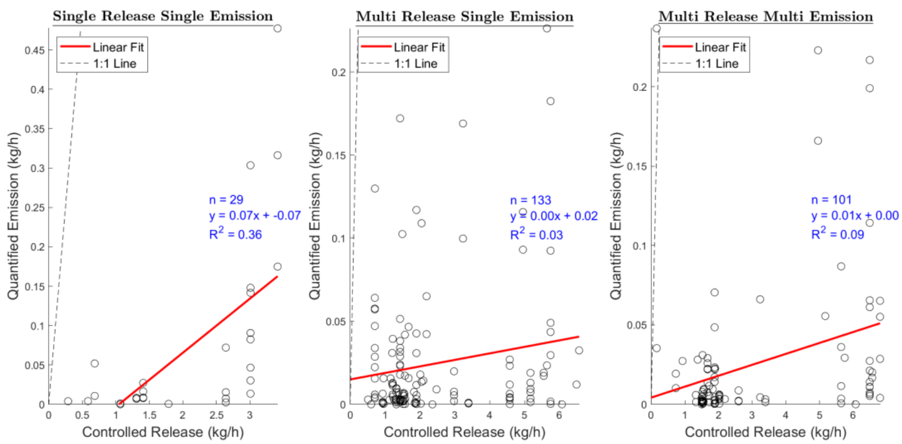

Figure 4: Quantified emission calculated using the eddy covariance method. Left pane shows a scatter plot of quantified emission versus total controlled release for a single release at the site level and the mast was downwind of the release point. Center pane shows a scatter plot of quantified emission versus total controlled release for multiple releases at the site level, but the mast was downwind of a single release point. Right pane shows a scatter plot of quantified emission versus total controlled release for multiple releases at the site level and the mast was downwind of more than one release point. The dashed line represents the 1:1 line (points below the line were underestimated), the red line is the linear regression fit of the data, and n is the number of data points.

https://doi.org/10.5194/egusphere-2024-3161
Preprint. Discussion started: 13 November 2024
© Author(s) 2024. CC BY 4.0 License.

3.1.2 Aerodynamic Flux Gradient

The aerodynamic flux gradient method also largely underestimated emissions for single release single emission, multi release single emission and multi release multi emission (Figure 5). A plot of quantified emission versus actual release did not show a linear relationship (R^2 between 0.01 and 0.39), and most data points were below the 1:1 line (Figure 5). The aerodynamic flux gradient quantified emissions were between 0 and about 1.6 kg h^{-1} despite actual emissions being between 0 and about 7 kg h $^{-1}$ (Figure 5). The underestimation was also consistent across all downwind ranges, 10, 20 and 30 degrees (Supplementary Material Section 2.2).

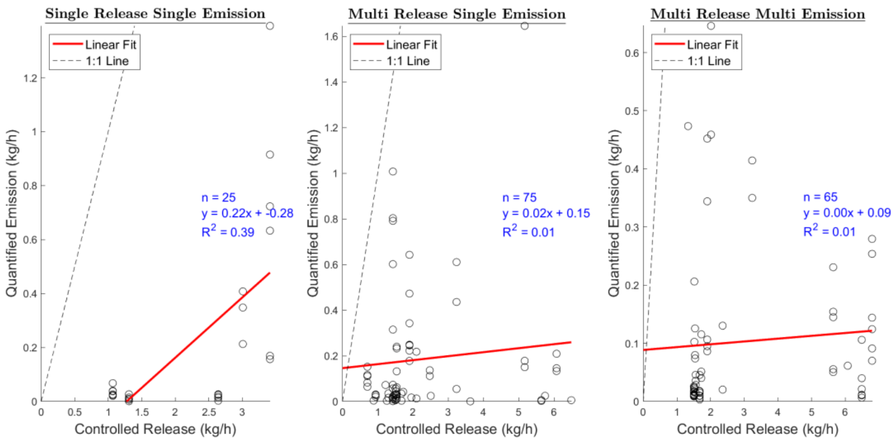

Figure 5: Quantified emission calculated using the aerodynamic flux gradient method. Left pane shows a scatter plot of quantified emission versus total controlled release for a single release at the site level and the mast was downwind of the release point. Center pane shows a scatter plot of quantified emission versus total controlled release for multiple releases at the site level, but the mast was downwind of a single release point. Right pane shows a scatter plot of quantified emission versus total controlled release for multiple releases at the site level and the mast was downwind of more than one release point. The dashed line represents the 1:1 line (points below the line were underestimated), the red line is the linear regression fit of the data, and n is the number of data points.

3.1.3 Gaussian Plume Inverse Method

The Gaussian plume inverse method was tested for single release single emission and multi release single emission as the method is only used for single-point sources and preliminary results showed the method provided reasonable results within 20 degrees downwind range (Figure 6; Supplementary Material Section 1.3). For single release single emission, the method quantified emissions within a factor of 1.5 (Figure 6) and showed reasonably linear relationship (R^2 of 0.65) (Figure 6). For multi release single emission, the gradient (m) of the linear regression was 0.95 and R^2 of 0.21. This suggests that the linear relationship cannot be well explained due to a random scatter of calculated emissions.

https://doi.org/10.5194/egusphere-2024-3161
Preprint. Discussion started: 13 November 2024
© Author(s) 2024. CC BY 4.0 License.

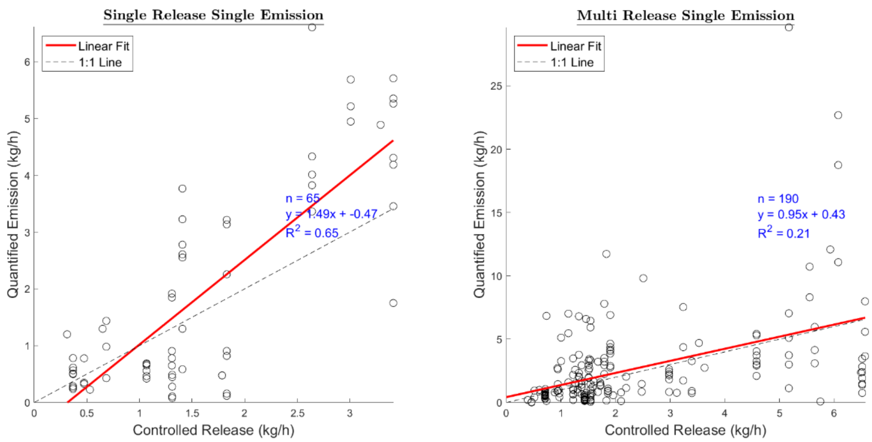

Figure 6*:* Quantified emission calculated using the Gaussian plume inverse method. Left pane shows a scatter plot of quantified emission versus total controlled release for a single release at the site level and the mast was downwind of the release point. Right pane shows a scatter plot of quantified emission versus total controlled release for multiple releases at the site level, but the mast was downwind of a single release point. The dashed line represents the 1:1 line (points below the line were underestimated), the red line is the linear regression fit of the data, and n is the number of data points.

3.2 Quantification within 30% Uncertainty

3.2.1 Eddy Covariance

The eddy covariance method showed a very low probability of quantifying emissions within 30% uncertainty (± 30%) (Figure 7). Only a single measurement in the multi release multi emission category showed an approximately 0.01 probability of quantifying within 30% (Figure 7). The errors for eddy covariance were between -100 and -86% for single release single emission, between -100 and -82% for multi release single emission, and between -100 and about +30% for multi release multi emission (Figure 7). This shows that using eddy covariance to quantify single-point and multi-point emissions will largely underestimate emissions.

https://doi.org/10.5194/egusphere-2024-3161
Preprint. Discussion started: 13 November 2024
© Author(s) 2024. CC BY 4.0 License.

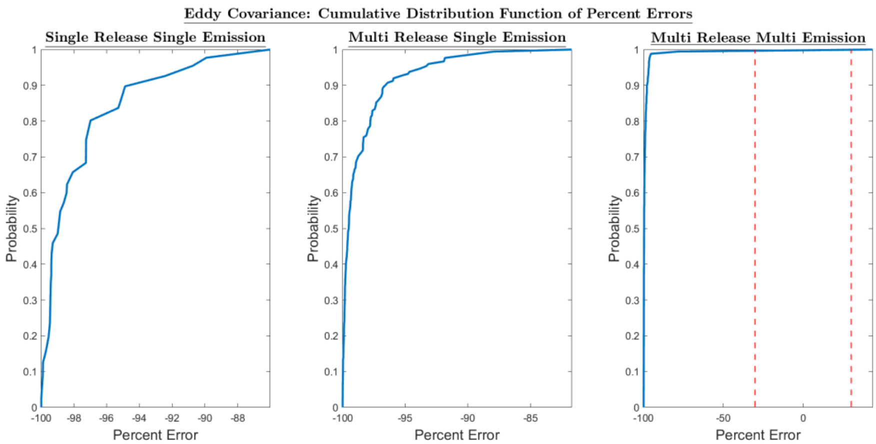

Figure 7: Cumulative distribution function (cdf) of percent errors for eddy covariance. Left pane shows a cdf plot for a single release at the site level and the mast was downwind of the release point. Center pane shows a cdf for multiple releases at the site level, but the mast was downwind of a single release point. Right pane shows a cdf for multiple releases at the site level and the mast was downwind of more than one release point. The area bounded by the red dotted line shows the region within ±30 uncertainty.

3.2.2 Aerodynamic Flux Gradient

The aerodynamic flux gradient also showed a very low probability of quantifying within 30% uncertainty (Figure 8). In the multi release single emission category results indicate a 0.02 probability of quantifying within 30% (Figure 8) of the true value. The errors for aerodynamic flux gradient were between -100 and -60% for single release single emission, between -100 and 0% for multi release single emission, and between -100 and -70% for multi release multi emission (Figure 8). These data show that the aerodynamic flux gradient will underestimate a point emission. Similar to eddy covariance, quantifying an emission within 30% uncertainty using aerodynamic flux gradient for point sources is highly unlikely.

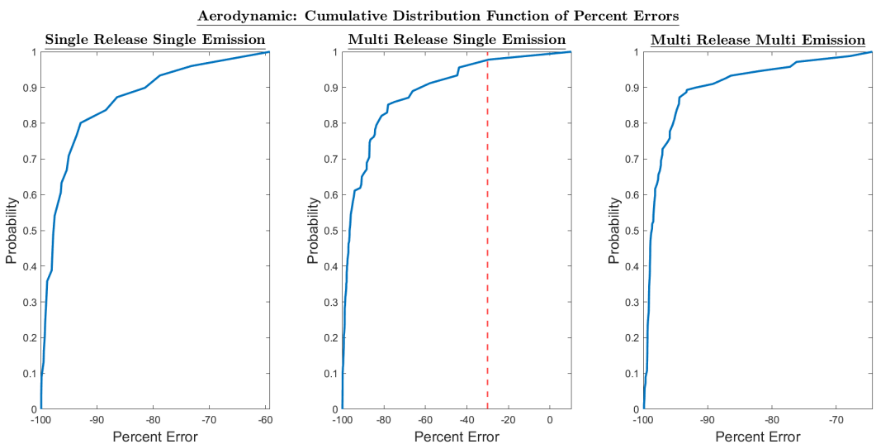

Figure 8: Cumulative distribution function (cdf) of percent errors for aerodynamic flux gradient method. Left pane shows a cdf plot for a single release at the site level and the mast was downwind of the release point. Center pane

https://doi.org/10.5194/egusphere-2024-3161
Preprint. Discussion started: 13 November 2024
© Author(s) 2024. CC BY 4.0 License.

shows a cdf for multiple releases at the site level, but the mast was downwind of a single release point. Right pane shows a cdf for multiple releases at the site level and the mast was downwind of more than one release point. The area bounded by the red dotted line shows the region within ±30 uncertainty.

3.2.3 Gaussian Plume Inverse Method

The Gaussian plume inverse method showed a higher probability of quantifying an emission correctly within 30% uncertainty than eddy covariance and aerodynamic flux gradient methods (Figure 9); ≈0.12 for the single release single emission and ≈0.25 for the multi release single emission categories (Figure 9). Percent errors of the Gaussian method calculated emissions are between -100 and +250% for single release single emission and between -100 and +800% for multi release single emission (Figure 9). This shows that even though the Gaussian method is designed for point sources, it is highly likely to miss, underestimate or overestimate an emission. Similar to eddy covariance and aerodynamic flux gradient, it is a challenge to correctly quantify a single emission event (single release or multiple release) using the Gaussian plume inverse method.

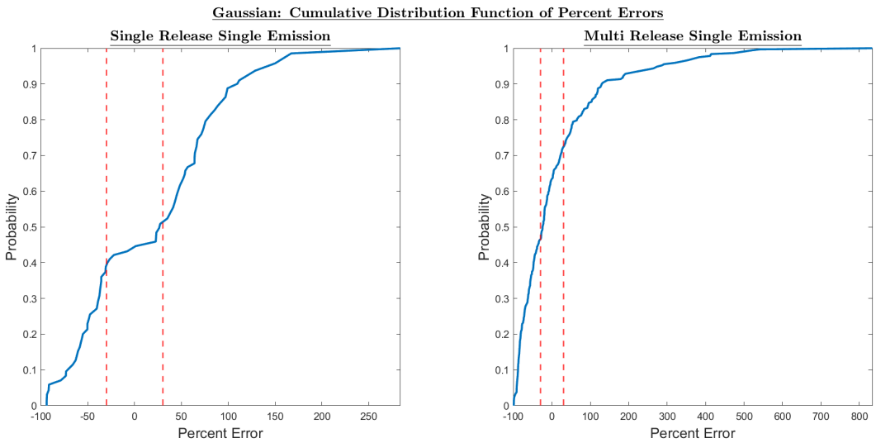

Figure 9: Cumulative distribution function (cdf) of percent errors for the Gaussian plume inverse method. Left pane shows a cdf for a single release at the site level and the mast was downwind of the release point. Right pane shows a cdf for multiple releases at the site level, but the mast was downwind of a single release point. The area bounded by the red dotted line shows the region within ±30 uncertainty.

3.3 Variables Affecting Quantification

3.3.1 Eddy Covariance

A Spearman's rank correlation analysis of measurement and environmental variables (distance, controlled release, emission height, mean wind speed (*WS*), Monin-Obukhov length (*L*) and contribution area) to percent error in quantification as calculated by the eddy covariance method, showed that downwind distance had significant impact on quantification for the single release single emission (p = 4.73e-6), multi release single emission (p = 2.66e-4), and multi release multi emission (p=2.00e-3) categories for $p < 0.01$ significance level (Figure 10). The correlation coefficients were -0.74 for single release single emission, -0.31 for multi release single emission, and -0.30 for multi release multi emission. The negative correlation in all three categories suggests that the percent error became more negative as distance increased i.e., far away emission sources were likely underestimated or undetected. Also,

https://doi.org/10.5194/egusphere-2024-3161
Preprint. Discussion started: 13 November 2024
© Author(s) 2024. CC BY 4.0 License.

controlled release and emission height had significant impact on quantification only in the multi release single emission category, p = 2.00e-3 and 9.42e-3 respectively, (Figure 10) but this correlation was inconsistent across the three categories. Due to inconsistent correlation, and the errors being close to -100%, the results show that generally, quantifying emissions using an eddy covariance approach will not work for emissions typically observed at oil and gas production sites.

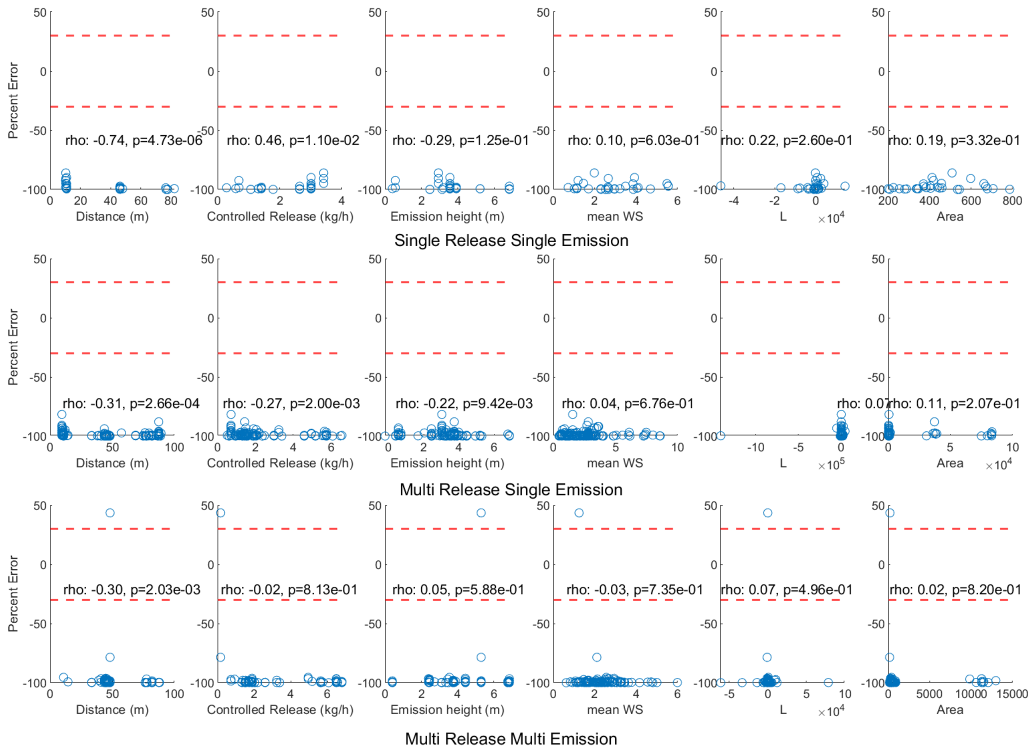

Figure 10: Correlation analysis for eddy covariance in the three release categories. The area bounded by the red dotted line shows the region within ±30 uncertainty.

3.3.2 Aerodynamic Flux Gradient

A Spearman's rank correlation analysis between the environmental and measurement variables and emissions calculated using the aerodynamic flux gradient method showed that only emission height in the single release single emission category had significant impact on model quantification (p = 1.79e-3) (Figure 11). The correlation between emission height and percent error in this category was -0.59 suggesting percent error became more negative as emission height increased. However, the correlation between emission height and percent error in the multi release single emission and multi release multi emission categories is approximately zero, meaning no correlation. Similar to eddy covariance, there is inconsistent correlation, and most errors are close to -100% (Figure 11). The results show that generally, quantifying emissions using an aerodynamic flux gradient approach will not work for emissions typically observed at oil and gas production sites.

https://doi.org/10.5194/egusphere-2024-3161
Preprint. Discussion started: 13 November 2024
© Author(s) 2024. CC BY 4.0 License.

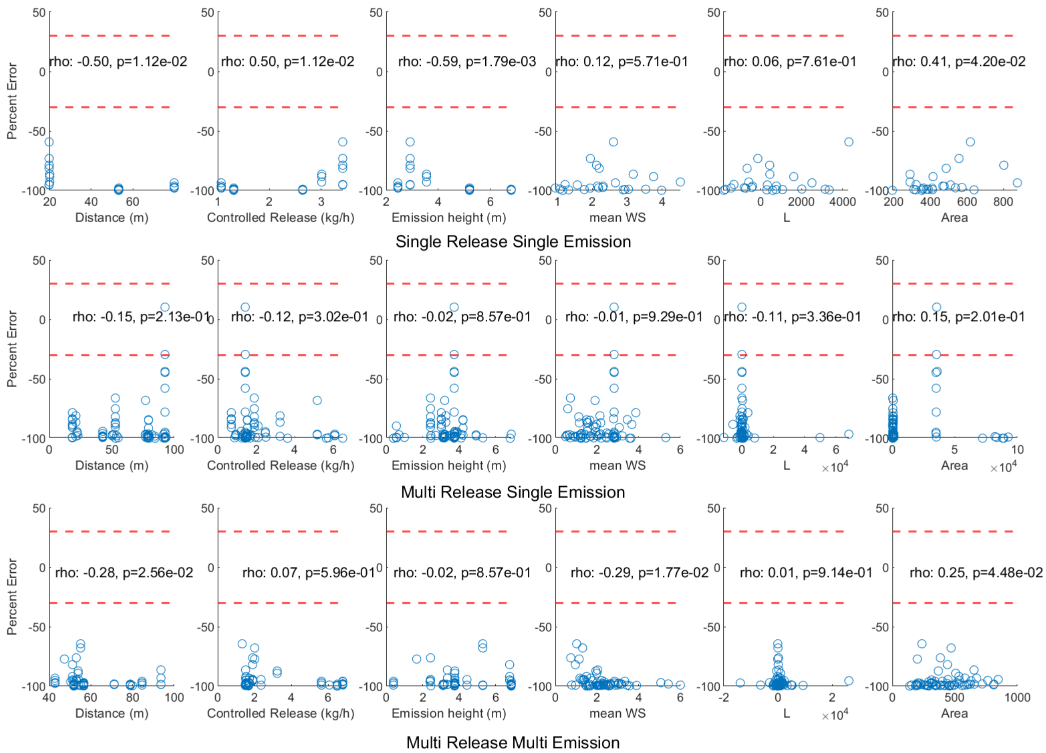

Figure 11: Correlation analysis for aerodynamic flux gradient in the three release categories. The area bounded by the red dotted line shows the region within ±30 uncertainty.

3.3.3 Gaussian Plume Inverse Method

The Spearman's rank correlation analysis between the emissions calculated using the Gaussian plume inverse method and measurement/environmental variables showed that only the mean wind speed and atmospheric stability had significant impact on the model quantification (Figure 12). In the single release single emission category, mean wind speed and percent error had a positive correlation (0.44, p = 2.74e-4) indicating that an increase in WS increased the model's positive error. However, in the multi release single emission category, the correlation is opposite (a negative correlation of -0.21, p = 3.71e-3) (Figure 12). Atmospheric stability had significant impact on model quantification in the multi release single emission category (p = 9.15e-5) but not in the single release single emission category (Figure 12). The correlation analysis for the Gaussian plume inverse model was inconsistent suggesting random errors in quantification. This shows that the model could either underestimate or overestimate an oil and gas emission at random.

https://doi.org/10.5194/egusphere-2024-3161
Preprint. Discussion started: 13 November 2024
© Author(s) 2024. CC BY 4.0 License.

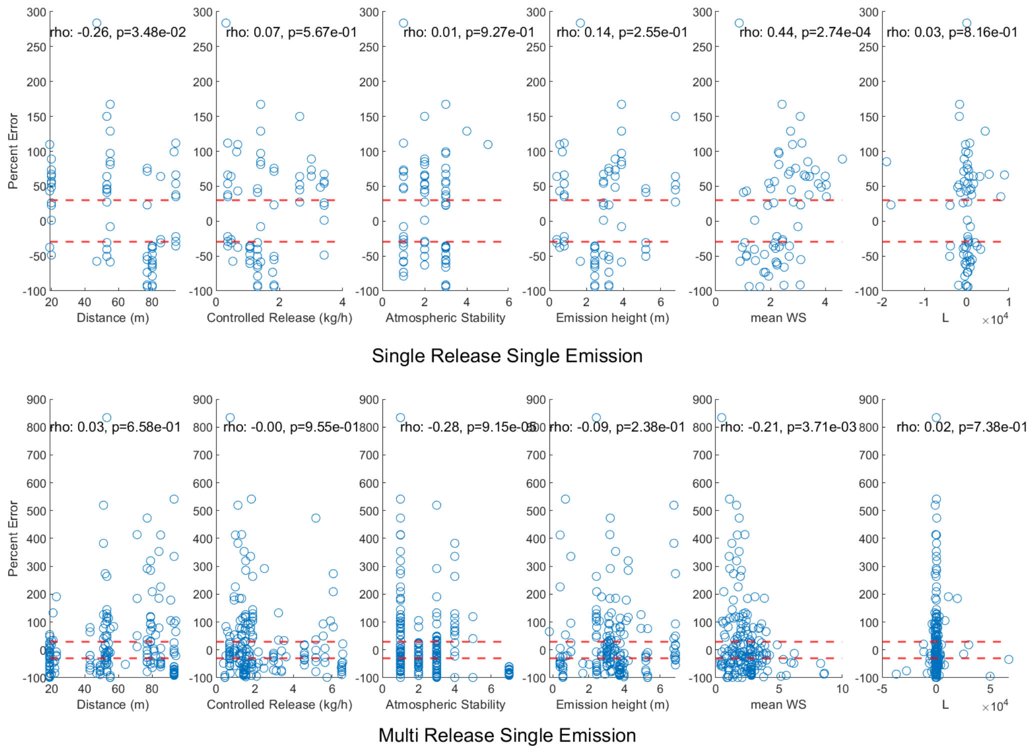

Figure 12: Correlation analysis for the Gaussian plume inverse method in the three release categories. The area bounded by the red dotted line shows the region within ±30 uncertainty.

4 Discussion

Methane emissions quantification from oil and gas is a complex system comprising of gas emissions from different heights, different locations, encountering aerodynamic obstacles of different sizes, and of varying duration, amongst others. The ability to precisely quantify an emission using data collected by a point sensor, downwind of a source is directly influenced by plume dynamics. The CH_4 plume downwind of a source will change in size and shape in different atmospheric conditions, in open areas versus areas with obstacles, diurnally, and in different seasons (Casal, 2008). In this study, the precision to which downwind models (eddy covariance, aerodynamic flux gradient and Gaussian plume-based) could quantify the emission rate of point source(s) were tested in different atmospheric conditions (rain, sunny, snow, windy, calm etc.), and aerodynamic scenarios (emissions sources in open areas, behind obstacles, changing atmospheric stability, and day/night). As a result, testing the models' predicted emission rates to controlled release rates in different conditions introduced real-world scenarios that have not previously been tested, hence better understanding model uncertainty in the application of quantifying emissions from oil and gas production infrastructure.

4.1 Eddy Covariance

Eddy covariance underestimated or failed to observe almost all emissions released during this study (linear regression m between 0 and 0.07, and R^2 between 0.03 and 0.36) (Figure 4). The method measures CH_4 atmospheric fluxes for

https://doi.org/10.5194/egusphere-2024-3161
Preprint. Discussion started: 13 November 2024
© Author(s) 2024. CC BY 4.0 License.

area sources transferred as eddies of different sizes as caused by turbulence within the atmospheric boundary layer (Babaeian and Tuller, 2023). Assumptions governing eddy covariance include: (1) the terrain is homogenous and horizontal, (2) CH_4 fluxes are turbulent, (3) measurements at a point are from an upwind area, (4) measurements are within the boundary layer and in the constant flux layer, (5) instruments can capture small fluctuations at high frequency, (6) fluctuations in air density are negligible (Babaeian and Tuller, 2023), and (7) upward fluxes represent emissions and downward fluxes represent depositions (Zinke et al., 2024). Nemitz et al., (2018) adds that eddy covariance is frequently deployed to target large fluxes in high-emission ecosystems, which is not typical in oil and gas, and that data where wind direction includes obstructed wind sectors should be flagged (Nemitz et al., 2018).

For oil and gas point sources, the measured gas concentration is dependent on plume dynamics as opposed to mass transfer and eddy covariance methods using fence-line measurements are unlikely to work because:

- Oil and gas point sources violate assumptions (1), (2), and (4) as these sources are heterogenous and emissions are collimated plumes instead of turbulent fluxes.
- As the measurement by a point sensor is dependent on being inside the plume, which changes in different atmospheric conditions, placing the sensor high enough, and/or far enough downwind, to where the flux layer is constant, is impractical.
- Even though current eddy covariance application assumes the vertical flux at a point is independent of atmospheric stability (Denmead, 2008), atmospheric stability has impact on point source gas dispersion at fence line distances and hence needs to be accounted for even for eddy measurements.
- Footprint models are designed for area sources that require horizontal homogeneity of the flow (Kljun et al., 2015). As a result, the area of contribution generated by the models do not accurately represent the area between the point sources and the measurement location at fence line distances.

In summary, this study shows that eddy covariance is not applicable for oil and gas point source quantification.

4.2 Aerodynamic Flux Gradient

Overall, aerodynamic flux gradient method underestimated the emission rate of all controlled releases during this experiment with high variability. The slope of the linear regression and R^2 were both very small (linear regression m between 0 and 0.22, and R^2 between 0.01 and 0.39) (Figure 5). The aerodynamic flux gradient model quantification is used to quantify emissions from area sources and relies on differences in CH_4 concentrations between the higher and lower height, and stability correction factors. Assumptions of flux-gradient approach using Monin-Obukhov similarity theory include: (1) measurements require steady state conditions of wind direction and speed, (2) measurements should be done above the roughness sub-layer, (3) sufficiently large homogenous area for development of an adequately equilibrated layer of air, and for constant equilibrium during measurement (Prueger and Kustas, 2015), and (4) positive fluxes represent emissions and downward fluxes represent absorptions (Kamp et al., 2020).

Similar to eddy covariance, aerodynamic flux gradient methods at fence-line distances are unlikely to work because point sources typical of oil and gas emissions violate the following assumptions:

- Obstacles at an oil and gas facility affects wind direction and speed, and these impacts may also vary substantially with small changes in wind direction. Therefore, wind conditions are unlikely to attain steady state during the measurement period, as directed by assumption (1) above.

- The emission height of oil and gas sources in typical upstream field conditions can be as low as 0.4 m and as high as 6.9 m and measurements are unlikely to be made by fence-line sensor above the roughness sublayer (2 above), i.e. twice the height of the mean obstacle height for ~30 m downwind.
- Oil and gas sources are heterogeneous (i.e. varying source distance and height) and can last a short time (e.g. a short maintenance event) or a long time (‘normal’ fugitive emissions) hence, achieving constant equilibrium, as stated in (3) above, is unlikely.
- Footprint models used to generate the area of contribution between the source and the measurement location are designed for area sources with horizontal flow homogeneity (Kljun et al., 2015). Thus, the area of contribution generated for oil and gas point sources is likely inaccurate.

4.3 Gaussian Plume Inverse Method

In contrast to the other methods in this study, the Gaussian plume inverse model both underestimated and overestimated emissions in this study. Linear regression gradient and coefficient of correlation (m between 0.95 and 1.49, and R^2 between 0.21 and 0.65; Figure 6) was better than either eddy covariance or aerodynamic flux gradient. The main assumption of the Gaussian plume model is that CH_4 emitted from a point source enters the air flow, disperses vertically and laterally, forming a conical plume (Riddick et al., 2022b; US EPA, 2013). However, the formation of a conical plume is hindered at oil and gas facilities by obstacles (equipment) and is affected by atmospheric stability. Atmospheric stability in the Gaussian plume inverse model is based on Pasquil-Gifford classification system which accounts for daytime solar insolation (slight, moderate and strong), nighttime cloud cover and surface wind speed at 10 m (Kahl and Chapman, 2018). Solar insolation and cloud cover are not typically measured, and if measured, dispersion parameter models currently available do not use this data, therefore, it is difficult to calculate for continuous fence-line measurements. The modified dispersion parameters developed by EPA (US EPA, 2013) only account for wind conditions i.e., speed and deviation in direction. As a result, plume dynamics during diverse atmospheric conditions such as during snow versus rain or sunny conditions are unaccounted for.

In this study, despite the Gaussian model having been developed for point sources, the model did not show consistent correlation with the measurement and atmospheric variables. This showed that there are complexities in continuous monitoring quantification compared to survey solutions where the model is widely applied, that introduce significant uncertainties in quantification. It is suggested that one problem with the Gaussian plume model is that the dispersion coefficients are simply not representative as they were developed for longer distances, in different climatological conditions, and do not transfer well to current applications (Riddick et al., 2022a). We conclude that, while it is better suited than eddy covariance or aerodynamic flux gradient, a Gaussian plume inverse approach will likely have significant uncertainties when used to quantify emissions from oil and gas production sites using data collected at a fence line (~ 30 m away).

4.4 Implications

In the recent years, there has been growing interest and need for accurate CH_4 quantification from oil and gas sites. This is generally done through survey methods and continuous monitoring using fence-line sensors. Continuous monitoring involves having stationary sensors measuring meteorology and CH_4 mixing ratios, which are then used to infer emission rate. For point sources, downwind methods such as the Gaussian plume inverse method have been

https://doi.org/10.5194/egusphere-2024-3161
Preprint. Discussion started: 13 November 2024
© Author(s) 2024. CC BY 4.0 License.

widely used, especially for survey quantification. Continuous monitoring is relatively new but fast growing. This study's design replicated a continuous monitoring setup.

Oil and gas point sources could either be single emissions or multiple emissions occurring concurrently. In cases of multiple emissions with more than one release point being downwind, the Gaussian model is limited, as it can only quantify one source at a time (dispersion coefficients are generated as a function of emission height and source distance). As a result, models used in other applications such as eddy covariance and aerodynamic flux gradient have been proposed as the solution. However, as this study has shown, eddy covariance and flux gradient approaches are unlikely to quantify realistic emission estimates using fence-line measurements. Here, we strongly advise that controlled tests under controlled environments are crucial to evaluate modelling approaches' precision and accuracy, and associated uncertainties before applying them in the real world. Even though these modelling approaches have been reported to work elsewhere (e.g., agricultural and landfill emissions), it does not necessary mean it could work in the intended area of application.

Author contributions

Mercy Mbua: Conceptualization, Data curation, Methodology, Formal analysis, Investigation, Writing original draft, Review, and Editing. Stuart N. Riddick: Conceptualization, Methodology, Review, Editing, Project Administration, Supervision, and Funding Acquisition. Elijah Kiplimo: Investigation, Review, and Editing. Daniel J. Zimmerle: Review, Editing, Funding acquisition, and Project administration.

Declaration of competing interest

The authors declare that they have no known competing financial interests or personal relationships that could have appeared to influence the work reported in this paper.

Acknowledgment

This work is funded by the Office of Fossil Energy and Carbon Management within the Department of Energy as part of the Site-Air-Basin Emissions Reconciliation (SABER) Project #DE-FE0032288. Any opinions, findings, conclusions, or recommendations expressed herein are those of the authors and do not necessarily reflect the views of those providing technical input or financial support. The trade names mentioned herein are merely for identification purposes and do not constitute an endorsement by any entity involved in this study. The authors also thank Ryan Brouwer, Daniel Fleischmann, Ryan Buenger, and Wendy Hartzell for their assistance.

Data availability

Data sets for this research are available in the in-text data citation reference: Mercy, Mbua; Riddick, Stuart N.; Kiplimo, Elijah, and Zimmerle, Daniel J. Dataset for evaluating the accuracy of downwind methods for quantifying point source emissions. [Dataset]. Dyrad.

References

Babaeian, E., Tuller, M., 2023. Proximal sensing of evapotranspiration, in: Encyclopedia of Soils in the Environment. Elsevier, pp. 610–617. https://doi.org/10.1016/B978-0-12-822974-3.00156-7

Bell, C., Ilonze, C., Duggan, A., Zimmerle, D., 2023. Performance of Continuous Emission Monitoring Solutions under a Single-Blind Controlled Testing Protocol. Environ. Sci. Technol. 57, 5794–5805. https://doi.org/10.1021/acs.est.2c09235

https://doi.org/10.5194/egusphere-2024-3161
Preprint. Discussion started: 13 November 2024
© Author(s) 2024. CC BY 4.0 License.

Brown, J.A., Harrison, M.R., Rufael, T., Roman-White, S.A., Ross, G.B., George, F.C., Zimmerle, D., 2023. Informing Methane Emissions Inventories Using Facility Aerial Measurements at Midstream Natural Gas Facilities. Environ. Sci. Technol. 57, 14539–14547. https://doi.org/10.1021/acs.est.3c01321

Carbon Mapper, 2024. Methane, CO2 Detection Satellite l Greenhouse Gas l Carbon Mapper [WWW Document]. Carbon Mapper. URL https://carbonmapper.org/ (accessed 2.26.24).

Casal, J., 2008. Chapter 6 Atmospheric dispersion of toxic or flammable clouds, in: Industrial Safety Series. Elsevier, pp. 195–248. https://doi.org/10.1016/S0921-9110(08)80008-0

Caulton, D.R., Li, Q., Bou-Zeid, E., Fitts, J.P., Golston, L.M., Pan, D., Lu, J., Lane, H.M., Buchholz, B., Guo, X., McSpiritt, J., Wendt, L., Zondlo, M.A., 2018. Quantifying uncertainties from mobile-laboratory-derived emissions of well pads using inverse Gaussian methods. Atmospheric Chem. Phys. 18, 15145–15168. https://doi.org/10.5194/acp-18-15145-2018

Caulton, D.R., Shepson, P.B., Santoro, R.L., Sparks, J.P., Howarth, R.W., Ingraffea, A.R., Cambaliza, M.O.L., Sweeney, C., Karion, A., Davis, K.J., Stirm, B.H., Montzka, S.A., Miller, B.R., 2014. Toward a better understanding and quantification of methane emissions from shale gas development. Proc. Natl. Acad. Sci. 111, 6237–6242. https://doi.org/10.1073/pnas.1316546111

CCAC, 2024. Climate and Clean Air Coalition | Homepage | Climate & Clean Air Coalition [WWW Document]. URL https://www.ccacoalition.org/ (accessed 8.15.24).

Chung, T., 2021. Global Assessment: Urgent Steps Must Be Taken to Reduce Methane Emissions This Decade | UNFCCC [WWW Document]. URL https://unfccc.int/news/global-assessment-urgent-steps-must-be-taken-to-reduce-methane-emissions-this-decade (accessed 10.23.23).

CO2EFFICIENT, 2022. METHANE QUANTIFICATION: TOWARD DIFFERENTIATED GAS [WWW Document]. CO2E. URL https://co2efficient.com/methane (accessed 2.11.24).

Colorado State University, 2021. Mechanistic Emission Estimation Tool (MEET) [WWW Document]. Energy Inst. URL https://energy.colostate.edu/mechanistic-air-emissions-simulator/ (accessed 2.26.24).

Conrad, B.M., Tyner, D.R., Johnson, M.R., 2023. Robust probabilities of detection and quantification uncertainty for aerial methane detection: Examples for three airborne technologies. Remote Sens. Environ. 288, 113499. https://doi.org/10.1016/j.rse.2023.113499

Crenna, B., 2006. An introduction to WindTrax.

Day, R.E., Emerson, E., Bell, C., Zimmerle, D., 2024. Point Sensor Networks Struggle to Detect and Quantify Short Controlled Releases at Oil and Gas Sites. Sensors 24, 2419. https://doi.org/10.3390/s24082419

Denmead, O.T., 2008. Approaches to measuring fluxes of methane and nitrous oxide between landscapes and the atmosphere. Plant Soil 309, 5–24. https://doi.org/10.1007/s11104-008-9599-z

Edie, R., Robertson, A.M., Field, R.A., Soltis, J., Snare, D.A., Zimmerle, D., Bell, C.S., Vaughn, T.L., Murphy, S.M., 2020. Constraining the accuracy of flux estimates using OTM 33A. Atmospheric Meas. Tech. 13, 341–353. https://doi.org/10.5194/amt-13-341-2020

Foster-Wittig, T.A., Thoma, E.D., Albertson, J.D., 2015. Estimation of point source fugitive emission rates from a single sensor time series: A conditionally-sampled Gaussian plume reconstruction. Atmos. Environ. 115, 101–109. https://doi.org/10.1016/j.atmosenv.2015.05.042

Heimburger, A.M.F., Harvey, R.M., Shepson, P.B., Stirm, B.H., Gore, C., Turnbull, J., Cambaliza, M.O.L., Salmon, O.E., Kerlo, A.-E.M., Lavoie, T.N., Davis, K.J., Lauvaux, T., Karion, A., Sweeney, C., Brewer, W.A., Hardesty, R.M., Gurney, K.R., 2017. Assessing the optimized precision of the aircraft mass balance method for measurement of urban greenhouse gas emission rates through averaging. Elem. Sci. Anthr. 5, 26. https://doi.org/10.1525/elementa.134

Hutchinson, M., Oh, H., Chen, W.-H., 2017. A review of source term estimation methods for atmospheric dispersion events using static or mobile sensors. Inf. Fusion 36, 130–148. https://doi.org/10.1016/j.inffus.2016.11.010

Ilonze, C., Emerson, E., Duggan, A., Zimmerle, D., 2024. Assessing the Progress of the Performance of Continuous Monitoring Solutions under a Single-Blind Controlled Testing Protocol. Environ. Sci. Technol. 58, 10941–10955. https://doi.org/10.1021/acs.est.3c08511

Jia, M., Daniels, W., Hammerling, D., 2023. Comparison of the Gaussian plume and puff atmospheric dispersion models on oil and gas facilities (preprint). Chemistry. https://doi.org/10.26434/chemrxiv-2023-hc95q

Kahl, J.D.W., Chapman, H.L., 2018. Atmospheric stability characterization using the Pasquill method: A critical evaluation. Atmos. Environ. 187, 196–209. https://doi.org/10.1016/j.atmosenv.2018.05.058

Kamp, J.N., Häni, C., Nyord, T., Feilberg, A., Sørensen, L.L., 2020. The Aerodynamic Gradient Method: Implications of Non-Simultaneous Measurements at Alternating Heights. Atmosphere 11, 1067. https://doi.org/10.3390/atmos11101067

https://doi.org/10.5194/egusphere-2024-3161
Preprint. Discussion started: 13 November 2024
© Author(s) 2024. CC BY 4.0 License.

Kljun, N., Calanca, P., Rotach, M.W., Schmid, H.P., 2015. A simple two-dimensional parameterisation for Flux Footprint Prediction (FFP). Geosci. Model Dev. 8, 3695–3713. https://doi.org/10.5194/gmd-8-3695-2015

METEC | Colorado State University [WWW Document], 2024. URL https://metec.colostate.edu/ (accessed 8.26.24).

Morin, T.H., 2019. Advances in the Eddy Covariance Approach to CH_4 Monitoring Over Two and a Half Decades. J. Geophys. Res. Biogeosciences 124, 453–460. https://doi.org/10.1029/2018JG004796

Nemitz, E., Mammarella, I., Ibrom, A., Aurela, M., Burba, G.G., Dengel, S., Gielen, B., Grelle, A., Heinesch, B., Herbst, M., Hörtnagl, L., Klemedtsson, L., Lindroth, A., Lohila, A., McDermitt, D.K., Meier, P., Merbold, L., Nelson, D., Nicolini, G., Nilsson, M.B., Peltola, O., Rinne, J., Zahniser, M., 2018. Standardisation of eddy-covariance flux measurements of methane and nitrous oxide. Int. Agrophysics 32, 517–549. https://doi.org/10.1515/intag-2017-0042

Prueger, J.H., Kustas, W.P., 2015. Aerodynamic Methods for Estimating Turbulent Fluxes, in: Hatfield, J.L., Baker, J.M. (Eds.), Agronomy Monographs. American Society of Agronomy, Crop Science Society of America, and Soil Science Society of America, Madison, WI, USA, pp. 407–436. https://doi.org/10.2134/agronmonogr47.c18

Querino, C.A.S., Smeets, C.J.P.P., Vigano, I., Holzinger, R., Moura, V., Gatti, L.V., Martinewski, A., Manzi, A.O., De Araújo, A.C., Röckmann, T., 2011. Methane flux, vertical gradient and mixing ratio measurements in a tropical forest. Atmospheric Chem. Phys. 11, 7943–7953. https://doi.org/10.5194/acp-11-7943-2011

Rey-Sanchez, C., Arias-Ortiz, A., Kasak, K., Chu, H., Szutu, D., Verfaillie, J., Baldocchi, D., 2022. Detecting Hot Spots of Methane Flux Using Footprint-Weighted Flux Maps. J. Geophys. Res. Biogeosciences 127, e2022JG006977. https://doi.org/10.1029/2022JG006977

Riddick, S.N., Ancona, R., Cheptonui, F., Bell, C.S., Duggan, A., Bennett, K.E., Zimmerle, D.J., 2022a. A cautionary report of calculating methane emissions using low-cost fence-line sensors. Elem. Sci. Anthr. 10, 00021. https://doi.org/10.1525/elementa.2022.00021

Riddick, S.N., Cheptonui, F., Yuan, K., Mbua, M., Day, R., Vaughn, T.L., Duggan, A., Bennett, K.E., Zimmerle, D.J., 2022b. Estimating Regional Methane Emission Factors from Energy and Agricultural Sector Sources Using a Portable Measurement System: Case Study of the Denver–Julesburg Basin. Sensors 22, 7410. https://doi.org/10.3390/s22197410

Riddick, S.N., Mauzerall, D.L., 2023. Likely substantial underestimation of reported methane emissions from United Kingdom upstream oil and gas activities. Energy Environ. Sci. 16, 295–304. https://doi.org/10.1039/D2EE03072A

Riddick, S.N., Mauzerall, D.L., Celia, M., Allen, G., Pitt, J., Kang, M., Riddick, J.C., 2020. The calibration and deployment of a low-cost methane sensor. Atmos. Environ. 230, 117440. https://doi.org/10.1016/j.atmosenv.2020.117440

Riddick, S.N., Mbua, M., Anand, A., Kiplimo, E., Santos, A., Upreti, A., Zimmerle, D.J., 2024a. Estimating Total Methane Emissions from the Denver-Julesburg Basin Using Bottom-Up Approaches. Gases 4, 236–252. https://doi.org/10.3390/gases4030014

Riddick, S.N., Mbua, M., Santos, A., Hartzell, W., Zimmerle, D.J., 2024b. Potential Underestimate in Reported Bottom-up Methane Emissions from Oil and Gas Operations in the Delaware Basin. Atmosphere 15, 202. https://doi.org/10.3390/atmos15020202

R.M. Young Company, 2023. . Ultrason. Anemometer Model 81000. URL https://www.youngusa.com/wp-content/uploads/2008/01/81000-9028I29.pdf

Shaw, J.T., Shah, A., Yong, H., Allen, G., 2021. Methods for quantifying methane emissions using unmanned aerial vehicles: a review. Philos. Trans. R. Soc. Math. Phys. Eng. Sci. 379, 20200450. https://doi.org/10.1098/rsta.2020.0450

Sonderfeld, H., Bösch, H., Jeanjean, A.P.R., Riddick, S.N., Allen, G., Ars, S., Davies, S., Harris, N., Humpage, N., Leigh, R., Pitt, J., 2017. CH₄ emission estimates from an active landfill site inferred from a combined approach of CFD modelling and in situ FTIR measurements. Atmospheric Meas. Tech. 10, 3931–3946. https://doi.org/10.5194/amt-10-3931-2017

Stull, R.B., 1988. An Introduction to Boundary Layer Meteorology, 1988 edition. ed, Atmospheric and Oceanographic Sciences Library. Springer Nature, Dordrecht. https://doi.org/10.1007/978-94-009-3027-8

UN Environment Programme, 2024. UNEP - UN Environment Programme [WWW Document]. URL https://www.unep.org/node (accessed 8.15.24).

United Nations Climate Change, 2015. Adoption of the Paris Agreement. Proposal by the President. | UNFCCC [WWW Document]. URL https://unfccc.int/documents/9064 (accessed 8.15.24).

US EPA, 2013. Standard Operating Procedure for Analysis of US EPA Geospatial Measurement of Air Pollution Remote Emission Quantification by Direct Assessment (GMAP-REQDA) Method Data for Methane

https://doi.org/10.5194/egusphere-2024-3161
Preprint. Discussion started: 13 November 2024
© Author(s) 2024. CC BY 4.0 License.

Emission Rate Quantification using the Point Source Gaussian Method [WWW Document]. URL https://www.epa.gov/sites/default/files/2020-08/documents/otm_33a_appendix_f1_psg_analysis_sop.pdf (accessed 5.6.24).

US EPA, OAR, 2023. Natural Gas and Petroleum Systems in the GHG Inventory: Additional Information on the 1990-2021 GHG Inventory (published April 2023) [WWW Document]. URL https://www.epa.gov/ghgemissions/natural-gas-and-petroleum-systems-ghg-inventory-additional-information-1990-2021-ghg (accessed 5.6.24).

US EPA, OA, 2023. Methane Emissions Reduction Program [WWW Document]. URL https://www.epa.gov/inflation-reduction-act/methane-emissions-reduction-program (accessed 1.16.24).

US EPA, O., 2016. Understanding Global Warming Potentials [WWW Document]. URL https://www.epa.gov/ghgemissions/understanding-global-warming-potentials (accessed 3.18.24).

Vogel, E., Davis, K.J., Wu, K., Miles, N.L., Richardson, S.J., Gurney, K.R., Monteiro, V., Roest, G.S., Kenion, H.C.R., Horne, J.P., 2024. Using eddy-covariance to measure the effects of COVID-19 restrictions on CO_2 emissions in a neighborhood of Indianapolis, IN. Carbon Manag. 15, 2365900. https://doi.org/10.1080/17583004.2024.2365900

Xu, L., Lin, X., Amen, J., Welding, K., McDermitt, D., 2014. Impact of changes in barometric pressure on landfill methane emission. Glob. Biogeochem. Cycles 28, 679–695. https://doi.org/10.1002/2013GB004571

Zimmerle, D., Dileep, S., Quinn, C., 2024. Unaddressed Uncertainties When Scaling Regional Aircraft Emission Surveys to Basin Emission Estimates. Environ. Sci. Technol. 58, 6575–6585. https://doi.org/10.1021/acs.est.3c08972

Zinke, J., Nilsson, E.D., Markuszewski, P., Zieger, P., Mårtensson, E.M., Rutgersson, A., Nilsson, E., Salter, M.E., 2024. Sea spray emissions from the Baltic Sea: comparison of aerosol eddy covariance fluxes and chamber-simulated sea spray emissions. Atmospheric Chem. Phys. 24, 1895–1918. https://doi.org/10.5194/acp-24-1895-2024